PHYSICAL REVIEW B VOLUME 48, NUMBER 18 1 NOVEMBER 1993-II

Electronic structure and stability of Ti-based $B2$ shape-memory compounds: X-ray and ultraviolet photoelectron spectra

Svetlana Shabalovskaya
Ames Laboratory and Department of Physics and Astronomy, Iowa State University, Ames, Iowa 50011

Alexander Narmonev
Central Research Institute of Black Metallurgy, Institute of Precise Alloys, Moscow, Russia

Olga Ivanova and Alexej Dementjev
All Union Research Centre of Surface and Vacuum, Moscow, Russia

(Received 10 July 1992; revised manuscript received 22 April 1993)

The evolution of x-ray photoelectron and ultraviolet spectra and their modification at the phase transformation $B2$-$B19$($B19'$) of equiatomic TiM and quasibinary Ti(Ni,M) compounds, where M stands for Fe, Co, Ni, Pd, Pt, Au, and Cu, are presented. Investigation of x-ray photoemission spectroscopy includes valence bands, satellites, and core-level energy studies. As the atomic number of M increases (both within the same period and along the group), its d states become more localized, the maximum and the center of gravity of the d bands shift towards the bottom of the valence band, and the M contribution to the density of states (DOS) at the Fermi level, $N(E_F)$, degrades. The DOS localization is accompanied by a spatial localization of the M d electrons resulting in weakening of the d-d covalent bonds between the alloy components and, thus, destabilizing the $B2$ phase. While the contribution of M d electrons to the DOS at E_F decreases, the Ti d electron portion increases to such an extent that, e.g., in TiPd and TiAu, the M contribution to $N(E_F)$ is almost negligible. The increase in core-level energy of all partners in compounds with respect to the elemental state is discussed in terms of covalency. The M d band localization leads to an increase of many-body interactions and, as a consequence, we managed to observe the Pd satellites without resonance enhancement. The $B2$-$B19'$ phase transition is accompanied by modification of the DOS which affects the Ti d states in general. Having analyzed the electronic structure we introduce parameters controlling the $B2$ phase stability and suggest a phenomenological formula for the martensitic-transformation temperature which satisfactorily describes the experimental behavior.

I. INTRODUCTION

In spite of intensive investigations of nitinol during the last 30 years it still remains a puzzle. Nitinol is remarkable not only for the shape memory effect, which continues to demonstrate new properties, but also for many phase transformations. What is the nature of such great variety? What contributions stabilize the high-temperature phase and what are the mechanisms of phase transformations? One may believe that the nature of the premartensitic phenomena in TiNi-based alloys has been understood today. It has been suggested[1,2] and later verified[3,4] that it is connected with charge-density waves. The nature of other phase transformations is yet to be revealed.

It is known the $B2$ structure is maintained by the total substitution of the isoelectronic analogous Pd and Pt for Ni. However, in this case this structure exists only at temperatures higher than 900 K. It is remarkable that the effect of Au is similar to that of Pd and Pt. On the other hand Cu, in contrast to Au, practically does not change the temperature of the martensitic transformation. In quasibinary Ti(Ni,Au) compounds the $B2$ phase exists throughout the whole range of Au concentration but in Ti(Ni,Cu) alloys it occurs only up to Cu concentrations of 30 at. %. In spite of the fact that Ag is isoelectronic to Cu and Au, it does not mix with TiNi at all. Substitution of transition metals, Co or Fe, for Ni gradually suppresses all phase transformations. So, in TiCo the martensitic $B2$-$B19$ transformation temperature, M_s is about 40 K; TiFe is stable in $B2$ structure until 0 K. What is the nature of the $B2$ phase stability in TiFe and what happens with M atomic number variation?

The x-ray emission spectra of K, L, and M series of both partners,[5-11] X-ray photoelectron spectra[12,13] for TiNi, and also the theoretical calculations of the electronic density of states (DOS) for TiFe (Ref. 14) and TiNi (Ref. 15) were known. One would think that the picture of the valence-band structure could be reconstructed using these data. However, some results in Refs. 5-11 differ with the experimental results described here not only in interpretation, but in essence as well. For instance, the Ni $M_{2,3}$ bands[5,6] are quite different in shape. As for Ti L_3 bands, the increases of the concentration of Ni throughout the whole concentration range of Ti-Ni alloys leads to an enhancement of the intensity of the long-wave maximum and, according to another investigation,[8] to an enhancement of the high-energy edge. Besides, so far, there is no satisfactory explanation for the 40-60 % increase in L-band intensity of both partners which takes place passing from the metallic state to the compound.[9,10] The amount of the Ti $K\alpha_1$ line shift in TiNi (Ref. 11) is comparable to that in TiN and TiO, though the difference in electronegativity between Ti and Ni atoms is not so large as in the latter case. There was no opportunity to use the theoretical calculations to eliminate the contradictions because some of them were based on parameters taken from those experiments. Because of this, it has been impossible to get reliable information about the valence-band structure of Ti*M* compounds from the available experimental data and the theoretical calculations. We have performed investigations of the electronic structure of Ti*M* compounds using x-ray (XPS) and ultraviolet (UPS) photoelectron spectroscopy, presented in this paper, as well as Auger spectroscopy[16] and electron-positron annihilation.[17] The combination of the methods chosen helps us develop a complete picture about different aspects of both the electronic structure and the interatomic bond.

It turned out that the XPS of Ti-based compounds with late transition metals, like locally sensitive methods, provides preliminary information on the *d* density of *M* states because of great differences in the photoionization cross section of the two partners. UPS, excited by He I (20.21 eV) radiation in contrast to XPS, yield an imprint of the total DOS in the case of 3*d* compounds. The most important data provided by these two methods are the general structure of the valence bands, their width and the energy position of different sub-bands.

The core-level behavior seems to be the most difficult to comprehend. This is not surprising because the final core-level shift which we measure is a result of the competition between different contributions, the values of which are usually not known.

The investigation of satellites also revealed some unexpected results. We managed to observe the Pd 4*d* band and $3d_{5/2}$ core-level satellites which had been observed earlier only due to a resonance enhancement of the 4*p* threshold emission. As for Ni satellites, they seem to be a "shake up" on nature. Satellites together with Auger spectroscopy present information about both many-body interactions and valence-band structure.

Using the described spectroscopic methods mentioned above we have studied the electronic structure change at the martensitic transformation $B2$-$B19(B19')$ in binary and quasibinary Ti(Ni,*M*)-based compounds and have come to the conclusion that the electron contribution to the total-energy change may be the most important one.

Based on the original research we attempt to understand the earlier x-ray emission spectroscopy data which have not been satisfactorily explained and to analyze the different electronic structure calculations. Our main purpose is to acquire information concerning the interatomic bond and the stability of the $B2$ structure of Ti*M* compounds.

II. EXPERIMENTAL

Binary and ternary alloys were produced by fusing iodine titanium and electrolytic nickel, carbonic iron, and other metals with purity 99.999 in an electrolytic-arc furnace in helium atmosphere. Homogenization was ensured by sixfold fusion. Loss of weight was not larger than 0.1%. After spark erosion cutting, the surface of the samples was mechanically polished and then etched chemically. The composition of the alloys has been checked by x-ray fluorescence with accuracy 0.2%. Crystal structure attestation was made using x-ray diffraction. For all alloys the temperature dependence of the electrical resistivity has been investigated and the temperatures of phase transformations have been determined.

The nearly equiatomic TiNi alloy of composition $Ti_{50.2}Ni_{49.8}$ experiences direct martensitic transformation in the interval 353–318 K (the first temperature M_s and the second M_f mean the start and the finish of the phase transformation) by cooling and the reverse transformation by heating in the range 373–393 K (A_s and A_f, respectively). The phase transformation interval for the TiPd, TiAu, and Ti(Ni,Pt) alloys investigated is higher than 830 K. The phase-transformation temperatures for the intermediate quasibinary compounds studied increase passing from TiNi to Ti*M*.

The x-ray photoelectron spectra were recorded by means of a Hewlett-Packard 5950 A spectrometer with escape angle of 72°. Instead of ion-argon etching, which is used for samples cleaning in the original spectrometer, the samples have been cleaned with the help of a boron nitride scraper in the preparation chamber in vacuum 10^{-8} Torr.

The built-in vidicon was substituted with another one in which a Si target is used instead of a photocathode. As a result of this reconstruction, the recording time for the valence band was lowered from several hours to 20–40 min, but the spectrometer resolution decreased from 0.6 to 0.85 eV. The spectrometer distortion function, remained Gaussian in shape. The interstitial admixture level has been estimated using oxygen and carbon lines. The accuracy of the data was ensured by repeated recording of the spectra on the freshly prepared surface.

The XPS for TiFe and TiNi were recorded at room temperature. TiNi and the ternary alloys having phase transformations near 373 K have been investigated in high- and low-temperature states. As for TiPd, it should be pointed out that we failed to obtain the high-temperature ($T > 850$ K) XPS. During the exposure time (~ 30 min) which is required for the valence-band and core-level registration on the samples surface, carbide layers are formed which cause surface contamination and a distortion of the original spectra. Because of this situation we have recorded the low-temperature spectra for TiPd, TiAu, Ti(Ni,Pt) and other ternary noble-metal alloys and discuss them together with the high-temperature results for other compounds. Such consideration is quite correct because change of XPS of the valence band due to alloying is ten times stronger than that achieved by passing from one structural type to another.[12,13]

The UPS experiment was carried out using a standard "VG" spectrometer "CLAM-100." Data recording and processing were performed by a standard "VGS-1000" system. UPS spectra of the valence bands excited by He I (21.21 eV) were recorded in pulse-counting mode with the resolution of $\Delta E/E = 0.7\%$ and at steps of 0.05 eV. The escape angle of the photoelectron with respect to the surface was 70°.

The residual gas pressure in the vacuum chamber was not more than 1×10^{-8} Torr. Sample surfaces were cleaned in vacuum during ion-argon etching. Auger spectra of oxygen, carbon, and sulfur were recorded before and after exposition for control of surface contamination.

III. RESULTS AND INTERPRETATION

A. XPS of the valence bands of titanium compounds with 3*d*metals

Let us consider the titanium-based compounds with late 3*d* metals. Figure 1 shows the x-ray photoelectron spectra together with DOS curves. From the variety of existing theoretical calculations the self-consistent ones have been selected.[14,15,18] As can be seen further, these calculations are in better agreement with various experimental data. Comparison of XPS with the $N(E)$ curves shows the closest accordance in position, shape, and width is achieved in the case of TiFe. This agreement becomes even better after the subtraction of the inelastic-scattering background from XPS. Upon removing the background we can also estimate correctly the width at the base of the valence band (Fig. 2). It turned out that the width of the occupied portion of the valence band increases from 4.4 to 5.5 eV from TiNi, TiCo, to TiFe, i.e., as the *M d* band occupancy decreases. In TiNi we also observe the valence-band satellite at 8 eV.

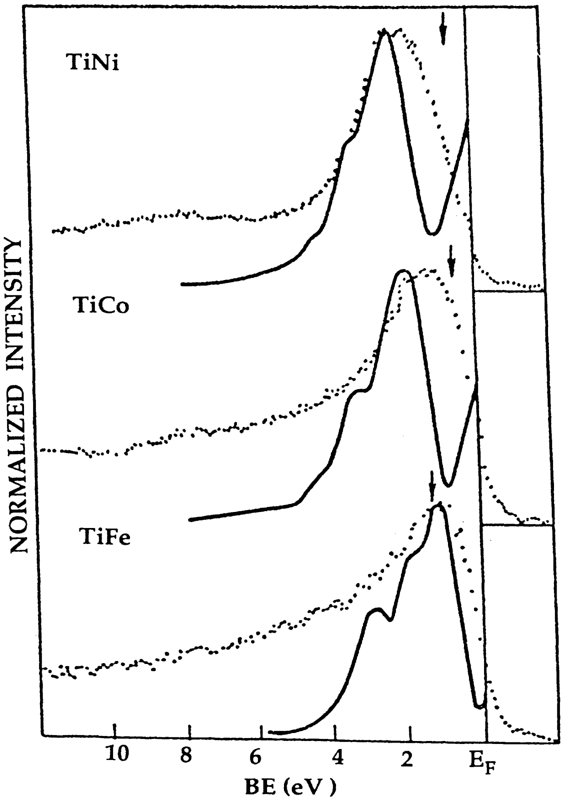

FIG. 1. Comparison of the observed XPS valence-band (VB) spectra with the calculated total DOS (Refs. 14, 15, and 18) broadened by 0.85-eV Gaussian function.

A cardinal difference in intensity at the Fermi level E_F is evident for TiNi. This disagreement might be due to the choice of an incorrect theoretical calculation. However, since in all known calculations the shape of total DOS coincides with that shown in Fig. 1, this explanation is probably not the best one. One may believe that the observed discrepancy is connected to the fact that XPS reflects the local DOS curve of one of the partners instead of the total one. Actually, by excitation of XPS with Al $K\alpha_1$ radiation we may neglect the probability of excitation of *s* and *p* states in comparison to that of *d* states. On the other hand, we know the photoelectron cross section of the Ti *d* states to be one to two orders of magnitude less than that of the late 3*d* transition metals.[19] Therefore, to a first approximation, the XPS of the studied compounds reproduce the shape of the local density of *M* states (Fig. 2). If it is so, the extraordinarily low XPS intensity at the Fermi level in TiNi indicates that the contribution of Ni *d* states to $N(E_F)$ is small. In this case the main portion of the $N(E_F)$ consists of the Ti *d* states. However, among well-known theoretical calculations there are those which actually predict that the Ti *d* state contribution[15,20–22] is dominant, as well as those suggesting the Ni *d* states dominate at the E_F.[23] In view of the above, one ought to recognize the latter calculations as incorrect. Thus, XPS of Ti compounds with late 3*d* metals may be used as a probe for the *M d* band investigation. This circumstance allows us to study the *M d*-band modification upon passing from an elemental state to a compound.

Let us demonstrate this on Ni (Fig. 3). The average width at half maximum of the TiNi *d* band is 2.8–3.0 eV. This practically coincides with the XPS of pure Ni. Note that XPS of all compounds presented here are 1.5–2 times narrower than the *L* and *M* x-ray emission spectra.[6–10] This circumstance becomes understandable considering that also *s* and *p* states contribute to the *L* and *M* bands, while XPS are determined predominantly by *d* states in the case of transition metals.

The major differences between Ni and TiNi XPS are as follows. (i) The increase of the energy of the main max-

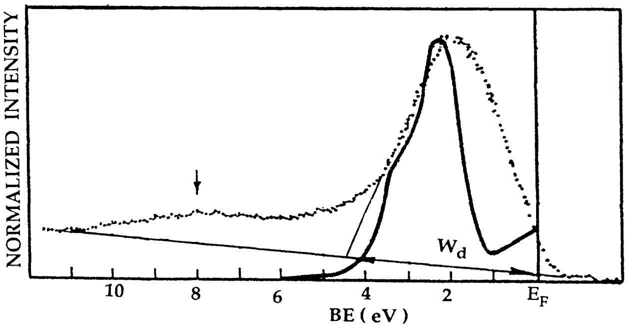

FIG. 2. XPS VB spectrum from Ni together with the local Ni *d* DOS (Ref. 15) broadened by 0.85-eV Gaussian function.

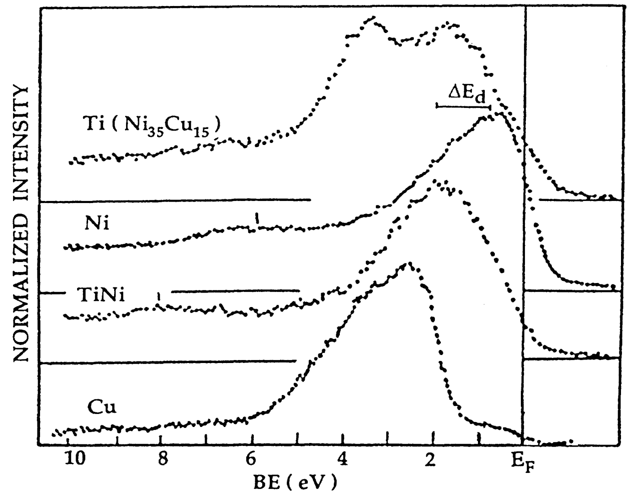

FIG. 3. XPS VB spectra from pure metals and their compounds. The Ni d band becomes Cu-like in TiNi. ΔE_d is the energy shift of the maximum of the M d band in compound with respect to that in the elemental state.

imum of the valence band relative to the Fermi level and accordingly the increase of the energy of the valence-band centroid by 1.3–1.5 eV, and (ii) the resulting decrease of intensity at the Fermi level. Comparison of TiNi XPS with that of Cu shows that the Ni d band becomes more symmetric and Cu like in this compound. This indicates, in our opinion, enhancement of Ni d electron localization in TiNi. The arrows in Fig. 1 show the location of the main maxima of XPS for the pure metals Ni, Co, Fe, and TiM compounds. The corresponding energy difference of the main XPS maxima of M in metallic state and in compound is denoted by ΔE_d. The Fe band peak position does not change passing from pure Fe to TiFe. Nevertheless, the intensity of TiFe XPS at the Fermi level decreases strongly in the compound.

Thus, it follows from the presented results that the M d band in Ti-based equiatomic compounds shifts to the bottom of the valence band in comparison with an elemental state. This is accompanied by the reduction of the M d states contribution to $N(E)$ in the vicinity of the Fermi level. If the Ti d states really dominate $N(E_F)$ then the observed M d-band shift indicates weakening of the d-d hybridization between partners in the E_F vicinity.

It is interesting that the Cu d band in Ti(Ni,Cu) alloys reveals a behavior similar to the d band of late transition metals. In alloys it shifts by ~1.0 eV relative to the elemental state, Fig. 3. We will discuss this result in Sec. III B.

B. The Ti compounds with 4d and 5d metals

Isoelectronic Pd or Pt and also the noble metal Au being substituted for Ni destabilize the $B2$ structure and increase the M_s temperature right up to the β-α allotropic transition temperature in pure Ti. Let us consider the valence-band evolution as the atomic number of the isoelectronic elements in Ti compounds increases. Note that the interpretation of XPS in terms of the dominant contribution of the M d band not only remains correct but becomes more justified as the photoelectron cross-section difference between Ti d electrons and those in 4d and 5d metals is greater than the cross-section difference between Ti d electron and those in the late 3d metals.[19]

Figure 4 shows the XPS of the valence bands of ternary Ti(Ni,Pd) alloys. The Pd substituting for Ni leads to the formation of a new subband with a maximum at about 4 eV whose intensity increases with the Pd content. Obviously this subband is caused by Pd d states. When the Pd content rises the 2-eV maximum decreases gradually and nearly disappears in binary TiPd. This confirms our interpretation of XPS of TiNi, according to which this structure is caused by the Ni d states. The clearly pronounced sub-band is located near E_F. One may think that this subtle structure reflects the Pd d states. However, the XPS investigation of Pd-Zr alloys (Zr is isoelectronic with Ti) over the whole composition range[24] indicate that this subband disappears as Zr concentration decreases. Therefore, the corresponding subband in TiPd is intrinsically connected with the Ti d states. There is one important point to note. The Pd d-band position does not change under composition variation in quasibinary compounds. On the other hand, passing from the elemental state to TiPd the Pd d-band maximum shifts by 2.5 eV to the bottom of the valence band. Under these circumstances the d-band width in the occupied part and in-

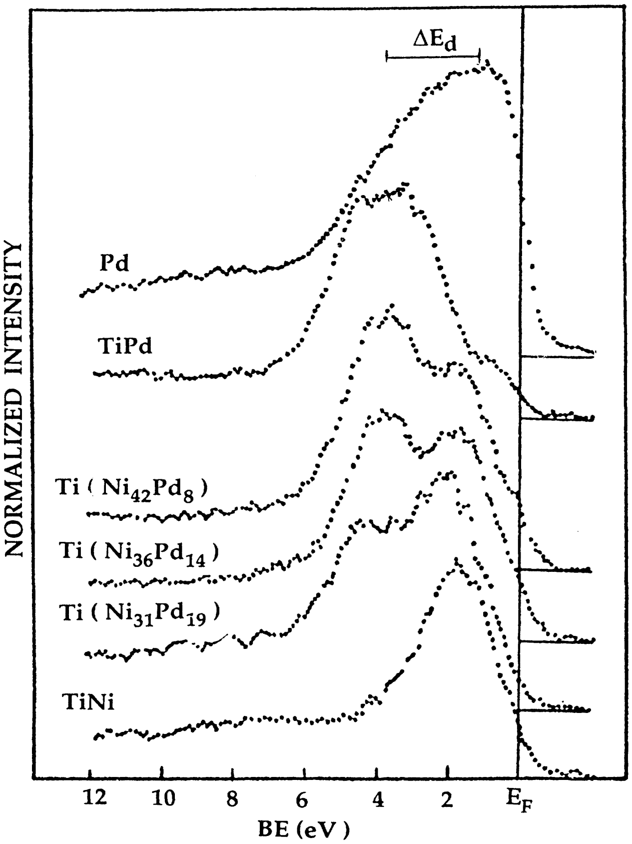

FIG. 4. XPS VB spectra from $Ti_{50}(Ni,Pd)_{50}$ compounds and Pd.

tensity at E_F considerably decrease. So the pure Pd has 4*d*-band width about 5 eV, while that of TiPd is 3.7 eV at the half maximum.

Investigation of Ti-based compounds with 5*d* metals showed that their *d* bands behave like those of Pd. Figure 5 presents the XPS of Ti(Ni,Pt) alloys together with that of pure Pt. After subtraction of the TiNi spectrum from the spectrum of the ternary alloy, superimposed at the Fermi level, one gets the Pt *d* band in the compound. It can be seen that the Pt *d* subband located near the Fermi level (*B* maximum) undergoes the largest change by alloying. The *A* maximum shift is only 1 eV and the shift of *B* is 2.6 eV. The Pt *d* band narrows to 3 eV at half maximum and acquires a Cu-like character with a low density of states at the Fermi level.

The narrowing, symmetrization and binding energy increase of Pd and Pt *d* bands in compounds shows a tendency toward atomization. Taking into account that the similar neighbors in the CsCl structure are the second ones and that their number decreases from 12 in the cubic face-centered lattice to 6 in the *B*2 structure, the *d*-band width behavior observed is not unexpected. We could suppose a similar behavior for *d* bands of 3*d* metals in Ti*M* compounds. However, in this last case the effect is rather opposite. The Ni *d*-band width does not change in TiNi but the Co and Fe *d*-band width in TiCo and TiFe actually increase. The lattice contraction observed passing from *M* to these compounds promotes the broadening of the Co and Fe *d* band, since the valence *d*-band width depends on the lattice parameter as $1/a^5$. However, it seems the lattice contraction is not enough to cause the positive sign of the observed effect. In the present case, the main factor competing with the decrease in number of neighbors and leading to the *d*-band broadening is the overlap of partner *d* bands, i.e., the covalent bond.

Thus, the increase of lattice contraction in the compounds TiNi, TiCo, and TiFe is a consequence of covalent bond strengthening and a reason for the *M* *d*-band width increase. The charge transfer to the *M* atoms, which has to increase passing from TiFe to TiNi, causes the Coulomb potential to extend the *d* bands of the components. A larger energy shift and narrowing of 4*d* and 5*d* bands in Ti*M* compounds may be a consequence of the latter.

Let us now discuss the quasibinary Ti(Ni,Au) alloys. Unlike Pd and Pt, which are isoelectronic to Ni, gold, as is commonly assumed by metallurgists, is a noble metal with a completely filled *d* band. However, its effect on the martensitic-transformation temperature in Ti(Ni,Au), in contrast to Cu, is similar to that of transition metals such as Pd or Pt. Now we try to understand the nature of those phenomena.

Figure 6 presents the XPS valence-band spectra of Ti(Ni,Au) alloys. By substituting Au for Ni, as in the case of Ti(Ni,Pd) alloys, the new band caused by the Au *d* states appears at ~6 eV. The intensity of the *d* band located in the vicinity of E_F drops with the reduction of Ni content and in TiAu only a plateau remains at that place. Note that the location of a new band's centroid does not change with composition variation as is the case for Ti(Ni,Pd) alloys. It is an unusual situation. For example, in Pd-Zr alloys[24] the Pd *d*-band maximum gradually shifts to the bottom of the valence band with the addition

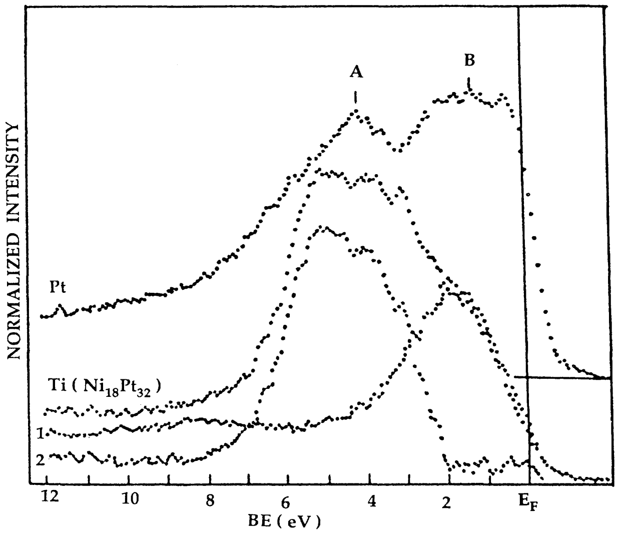

FIG. 5. XPS VB spectra from Pt, $Ti(Ni_{18}Pt_{32})$, and TiNi (1). Curve (2) presents the Pt *d* band in compound; it is the result of substraction of the TiNi spectrum from the spectrum of the compound.

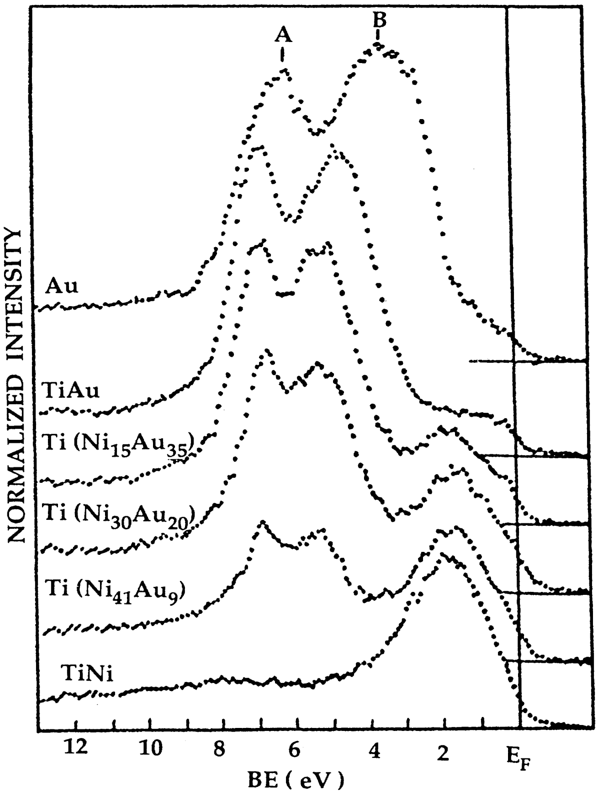

FIG. 6. XPS VB spectra from $Ti_{50}(Ni,Au)_{50}$ compounds and from Au.

of Zr until the near equiatomic composition is reached when similar Pd-Pd neighbors no longer exist. It seems the Pd *d*-band shifts with the change of the Pd nearest environment; consequently the *d*-band occupancy and interatomic bond change. If the Pd atoms extend into the second coordination sphere in Pd-Zr alloys the Pd *d*-band displacements become negligibly small. In the quasibinary compounds studied, the Pd and Au atoms substituting for Ni atoms have always been surrounded by Ti atoms. Thereby, the type of first neighbors of Ni, Pd, and Au atoms do not change versus composition and as a consequence the *d*-band energy of the second and the third components remains constant.

Let us return to Fig. 6. It is evident that the Au *d* band, centered near 6 eV, in fact, does not contribute to the $N\ (E_F)$. Note that its ~2 eV narrowing is caused mainly by the *B* sub-band. The *d*-band symmetrization and spin-orbit splitting decrease from 2.5 eV in pure Au to 1.6 eV in compounds are primarily the consequence of the *B* subband change. Apparently, the *d*-band narrowing and symmetrization indicate the strengthening of atomiclike character as a result of resettling of gold atoms into the second coordination sphere.

We can suppose, however, another mechanism which can also cause the strengthening of the atomiclike character of the Au *d* band. It is the increase of Au *d* band occupancy. As mentioned above, according to generally accepted assumption, gold has a completely filled *d* band. However, the wide asymmetric 5*d* band with large spin-orbit splitting contradicts this point of view. As it follows from the calculations of Mattheis and Deitz,[25] in elemental gold a subband exists in unfilled DOS region in the vicinity of E_F which has a *d* character as a result of *s*-*d* hybridization. According to this calculation, the electronic configuration of Au in the elemental state is the $5d^{9.6}6s^{0.9}6p^{0.5}$. This means that the *d* hole in metallic state is about 0.4 This is true for Cu as well, where the *d* hole is somewhat less (0.3).[26]

Based upon information on chemical compounds with known bond character we will try to gain some insight into the situation of the *d*-band occupancy in Ti*M* compounds. The authors in Ref. 26 present the XPS and Messbauer effect for AuZn, AuMg, AuRb, and AuCs. Passing from elemental state to these CsCl-type compounds the interatomic bond changes from metallic to ionic. For example, the AuCs is described as an ionic compound of Au^- and Cs^+. The isomer shift and core-level shifts show that the charge transfer from the second component to the Au atom increases from 0.2–0.3 to 1 electron per atom as the second component atomic number in compounds AuZn, AuRb, and AuCs. Thus, the last two compounds are ionic in nature. As the ionic contribution to the bond strengthens, the Au *d* band changes as it does in Ti(Ni,*M*) alloys. In AuMg, for instance, we observe an absolutely symmetric 5*d* band. The 1.5-eV spin-orbit splitting in AuCs is close to that in free Au ion and in Ti(Ni,Au) alloys. This similarity indicates that the Au *d*-band behavior in the latter case may also be due to *d*-band occupancy increase. Since the energy position and the width of the Au *d* band in AuZn coincides with that in Ti(Ni,Au) compounds, one can suppose an equal *d* charge increase of about 0.2–0.4 per Au atom. Thus, from the presented analysis, Au should be considered as a metal with unfilled *d* band and, as a result, its effect on the *B*2-*B*19(*B*19′) phase transformation in Ti(Ni,Au) is similar to that of Pd and Pt. The same is true for Cu.

C. Core level shifts

The core-level must provide the most direct information about the change of the character of the bonding by alloying. However, often it is very difficult to obtain this information. The total core-level shift includes three parts. The first is due to electronic configuration change. The second is the result of chemical environment variation (chemical shift) and the third is caused by relaxation energy change. As for the last contribution, this value is about 1 eV as one passes from a pure metal to an alloy. It can change in the range from 0.2 to 1.5 eV depending on the composition. The exact interpretation of core-level shifts requires elaborate computations. But sometimes even this level of computation does not ensure success. The authors in Ref. 27 using linear muffin-tin orbital–atomic-sphere approximation methods, managed to calculate core-level shifts in Ni-based alloys. But it turned out that the accuracy of those calculations was numerically identical to the value of shifts experimentally observed (~0.5 eV). Even when a charge transfer takes place there may be a balance between intratomic Coulomb shift caused by change in occupancy of *s*, *p*, and *d* states and interatomic Madelung contribution. Sometimes when the *s*, *p*, and *d* charges transfer in opposite directions the final shift may vanish.

Table I shows the energy shifts of the Ti $2p_{3/2}$ and *M* core levels relative to the metallic state. The binding en-

TABLE I. Core-level shifts in binary Ti*M* and quasibinary $\mathrm{Ti}_{50}(\mathrm{Ni},M)_{50}$ compounds (eV).

Compound core-level shifts	TiFe	TiCo	TiNi	$\mathrm{Ti(Ni_{25}Co_{25})}$		$\mathrm{Ti(Ni_{35}Cu_{15})}$		TiAu($4f_{7/2}$)	TiPd($3d_{5/2}$)	$\mathrm{Ti(Ni_{18}P_{32})}$	
Ti $2p_{3/2}$	0.2	0.4	0.5	0.2		0		0.7	0.9	0.6	
				Ni	Co	Ni	Cu			Ni	Pt($4f_{7/2}$)
Me $2p_{3/2}$	0.15	0	0.5	0.4	0	0.4	0	0.8	1.3	0.3	0.7
Ti $K\alpha_1^{a}$ shift (eV)	−0.190±0.007	−0.136±0.005	−0.062±0.003						+0.04±0.005		

[a] Reference 32.

ergy of the $2p_{3/2}$level of Ti is (454.3 ∓ 0.1) eV and that of Ni is (853 ∓ 0.1) eV. This seems to be in reasonable agreement with data obtained for TiNi in other investigations.[28,29]

Thus, the core-level energy of both partners when measured relative to the Fermi level increases in compounds. It is noteworthy that the Co and Cu $2p_{3/2}$ levels do not shift by alloying in titanium-based quasibinary compounds Ti(Ni,*M*) as is the case in Zr-based alloys.[30] Note that the binding energy of the valence bands also increases in Ti*M* compounds. But the valence-band peak displacements are twice as large as the core-level shifts. The similar sign of core-level shifts of both partners may be interpreted as a result of screening diminution caused by the drawing of charge from both components into interstitial sites. But taking into account that all shifts have been measured with respect to Fermi level, we have tried to recalculate them using electron work functions for pure metals (4.33; 5.15; 5.12 eV for Ti, Ni, and Pd, respectively[31]) with the assumption that the E_F of compounds is close to that of elemental Ti. As a result, the Ti core-level shifts keep their positive sign and value. The Ni $2p_{3/2}$ shift becomes negative $(-0.3$ eV) and the Pd $3d_{5/2}$ gets smaller, but remains positive (0.5 eV). This new situation enables us to suppose a charge transfer from Ti atoms to Ni in TiNi. However, based on these data we may not suggest any charge transfer from Ti to Pd atoms in TiPd.

In this context the Ti $K\alpha_1$ line shifts[32] are of great interest. These shifts, corresponding to energy difference change between 1*s* and 2*p* levels with respect to pure Ti, are also listed in Table I. In contrast to data presented by Källne,[11] their value is very small. As the metal atomic number increases, the initially negative Ti $K\alpha_1$ shift decreases gradually in absolute value becoming positive in TiPd. As it follows from investigations of chemical compounds,[33] the negative $K\alpha_1$ shifts indicate the diminution of total electron density of Ti atoms by alloying. Thus, the observed $K\alpha_1$ shift behavior shows that in TiFe, TiCo, and TiNi, the Ti atoms lose their charge. The latter process attenuates in this sequence of compounds and at last in TiPd the Ti sites become enriched with electrons. This is consistent with the core-level shift data according to which Ni and Pd reveal the different sign of core-level shifts. However, the negative Ti $K\alpha_1$ shift cannot be explained as charge transfer from Ti to *M* because, for example, the Fe $K\alpha_1$ shift is negative in TiFe as well $(-0.079 \mp 0.008$ eV).[32] Rather, negative shifts for both components mean the drawing off of electronic charge into interstitial sites as covalent bonding requires. Also the largest Ti $K\alpha_1$ shift in TiFe indicates the highest covalency among the investigated compounds. These results are in good agreement with maximal overlap of partner *d* bands in TiFe. Thus, the interpretation of core-level shifts in the case of intermetallic compounds where all kinds of bonds are present is not an easy task.

In the quasibinary Ti(Ni,*M*) compounds the core levels of second and third components as well as the valence band centroid position do not vary within the limits of experimental error. However, the Ti $2p_{3/2}$ level energy increases gradually with the concentration of the third component, as in Fig. 7. This very unusual partner core-level behavior can be explained taking into account that the *B*2 lattice is two cubic lattices one translated from the other. The first is occupied by Ti atoms and the second by *M* ones. In quasibinary compounds the Ti lattice remains unchanged and the sites of the second one are occupied by Ni and *M* atoms with equal probability. In view of this, the Ni and atoms of the third component have only Ti atoms as nearest neighbors and the environment of the Ti atoms changes from pure Ni to pure *M* by composition variation. As a result, we observe the unchanged core-level shift for Ni or *M* and the gradual variation of Ti 2*p* level shift versus composition. Such core-level behavior in quasibinary compounds means that the nearest neighbors have influence on the core-level shift. Also the Ti 2*p* level energy change indicates reorganization of the electronic density of Ti atoms due to the nearby environment. There is one important point to note: The Ti $2p_{3/2}$ energy increase upon passing from TiFe to TiNi, and to TiPd is in agreement with the increase of heat of formation of these compounds (20, 33, and 67 kJ/mol, respectively).[34]

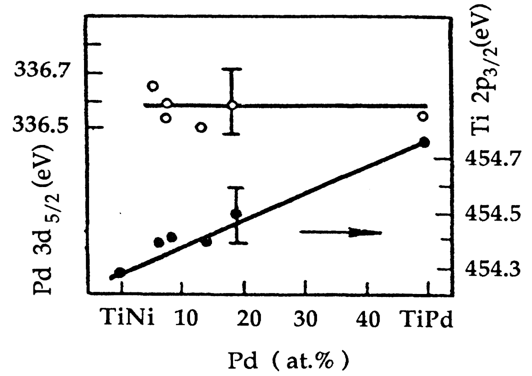

FIG. 7. Core-level shifts in quasibinary $Ti_{50}(Ni,Pd)_{50}$ compounds with respect to an elemental state.

D. The valence-band and core-level satellites

The strong localization character of *d* electrons and thereby the correlation effects cause ferromagnetism and satellite lines in the late 3*d* metals. The correlation effects are more pronounced in Ni, where the satellite intensity reaches approximately 30% of that of the main *d*-band peak. The d^9 and d^{10} configurations of Ni atoms are degenerate in the ground state. Upon photoionization of the valence band, the final state is the set of d^8 and d^9 configurations. The d^9 configuration corresponds to the state with a delocalized hole. But in the case of the d^8 configuration, both *d* holes are localized on the same atom. If the atomic Coulomb interaction between two *d* holes is of the order of several eV, then the electronic states corresponding to the configurations with the *d* holes of a different localization character will be separated. The energy separation between the main line and the satellite is U_{dd}—the energy of Coulomb interaction of two holes localized at the same atom. In the case of pure Ni it is ~ 5.7 eV.

The degeneration of d^9 and d^{10} configurations disappears when $2p$ core-level photoionization occurs as well. But in this case it is a result of the interaction of the $2p$ hole with the valence-band hole. A bound state of two holes appears when their interaction energy exceeds the d-band width. At the given d-band occupancy the appearance of satellites as well as their intensity depends on U/W value. At $U/W \geq 1$, there is a strong tendency toward satellite formation. On the other hand at given U_{dd} and W values the satellite intensity change indicates a corresponding change in d-band occupancy.

The Ni satellites are being considered as a result of a shake-up process[35] (i.e., the transition of photoelectrons into an excited state). In this case the satellite intensity is determined not only by the weight of the unoccupied part of the $3d$ band but also by the position of the latter with respect to E_F. The Ni $3d$ character, which is far above E_F, influences the satellite intensity less than an unfilled Ni $3d$ band with high density of states located immediately above the Fermi level.

Pd and Pt being the isoelectronic analogues of Ni have ~ 0.36 d hole in the valence band. However, under usual conditions they do not present satellites. As for Pd, its $4d$-band satellite has been observed only as a result of the resonance enhancement caused by photoexcitation of the threshold of $4p$ emission. This kind of enhancement takes place also in Ni when the excitation energies higher than 67 eV, i.e., when $3p$ emission has been initiated.

Let us now turn to our experimental results. The valence-band satellite of Ni is also observed in TiNi, Fig. 8. In the latter case its intensity decreases to 18% of the main d-band peak in comparison with the satellite in Ni. However, the energy separation between the satellite and the main d-band peak practically does not change.

In quasibinary Ti(Ni,*M*) alloys, where *M* is Pd, Pt, or Au the Ni $3d$ satellite cannot be observed because it overlaps with the heavy-metal d bands. But in these alloys, as in TiNi, we observe the Ni $2p_{3/2}$ satellite. Its intensity decreases to 14% of the main peak in Ti(Ni,*M*). By variation of the third component, its intensity fluctuates in the 10–15% interval. The energy separation between the $2p_{3/2}$ satellite and the main line is about 7–7.5 eV, Fig. 9. In contrast to pure Ni the latter value does not coincide with the energy separation of the valence-band satellite and the main line. We have no idea about the nature of difference between the energy position of the valence-band and core-level Ni satellites in TiNi. The reduction in intensity of the valence-band satellite which takes place at a constant U/W value indicates that these data should be considered as an argument for the shake-up nature of the Ni satellites. In this case the decrease of the satellite intensity is caused mainly by reconstruction of the valence band and degradation of the Ni d character in the vicinity of E_F in TiNi. This follows directly from the valence-band investigations.

It is remarkable that we managed to observe the Pd satellites in TiPd without any special conditions. The $4d$ satellite is located 12 eV below E_F. The energy separation between the satellite and the valence band is 9.0 eV, Fig. 8. That is 1.7 times larger than for pure Pd. The energy separation between the $3p_{3/2}$ satellite and the main line is the same as that of the valence-band satellite in contrast to the case of Ni satellite. The intensity of the 12-eV satellite is about 12% of that of the peak $4d$-band intensity. The registration of the Pd $4d$ satellite without resonance enhancement indicates a change of excitation conditions by alloying. In fact, going from pure Pd to TiPd we observe a 1.5× narrowing of the occupied part of valence band and a 1.7× increase of U_{dd}. As a result we observe a sharp increase of the U/W value which

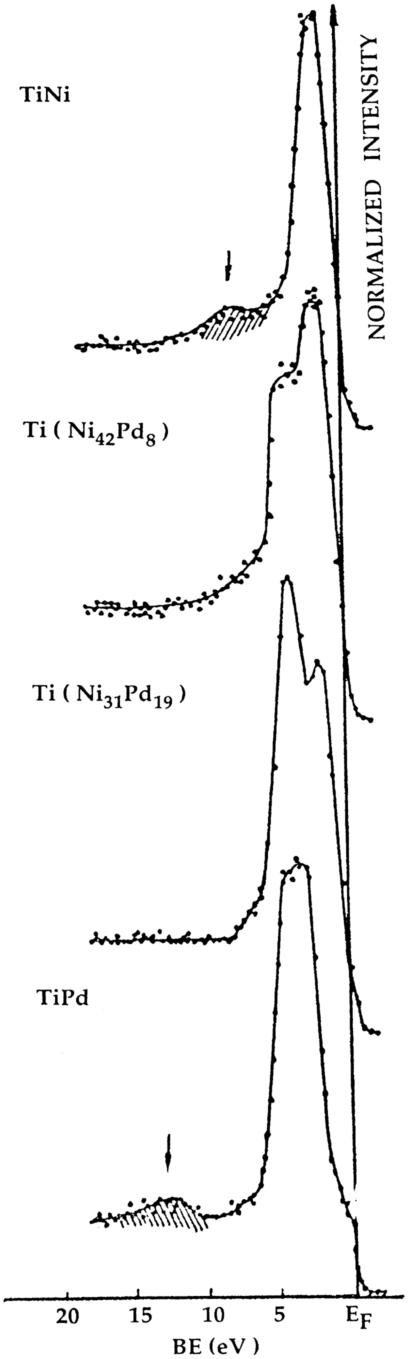

FIG. 8. VB satellites of Ni in TiNi and of Pd in TiPd.

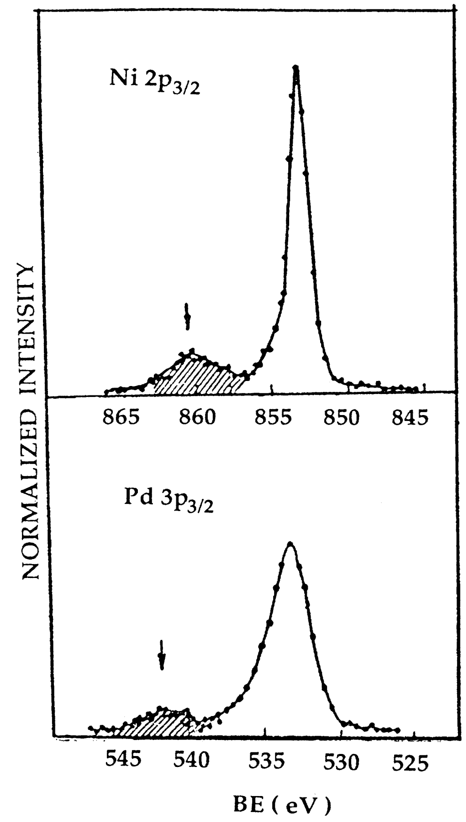

FIG. 9. Core-level satellites of Ni and Pd in TiNi and TiPd, respectively.

controls the character of *d* electron localization and satellite behavior. It is not out of place to note that the enhancement of hole interaction is itself a sign of Pd *d*-band localization strengthening which is in agreement with the valence-band research results presented above.

E. Ultraviolet photoelectron and x-ray emission spectroscopy

In the previous section the x-ray photoelectron spectra study of binary and quasibinary Ti-based compounds was discussed. The Ti *d* band does not develop in XPS because of the large difference in the *d* photoelectron cross section between Ti and late transition metals. More favorable for the study of the Ti *d* band is ultraviolet spectroscopy. However, as in the previous case where the photoelectron spectra are excited by low-energy photons, the UPS, in general, does not represent an imprint of the density-of-state curve. In addition to the photoelectron cross-section difference, the UPS shape is influenced by the structure of the unoccupied part of DOS. But the latter contribution is important only when the excitation energy is lower than 20 eV. In our case (He I=21.21 eV), while the binding energy of excited valence electrons does not exceed 4–6 eV, the photoelectron will have energy of about 15 eV, which significantly exceeds the bandwidth in the unoccupied part of the valence band. Thereby the structure of the $N(E)$ immediately above the Fermi level should not manifest itself in UPS. Another question we comment on below about the surface sensitivity of UPS.

Figure 10 shows the UPS excited by HeI radiation. In TiFe and TiCo samples whose surfaces were subjected only to ionic etching without a preliminary chemical etching, the 2*p* band of oxygen is pronounced in spectra as its photoelectron cross section is comparable to that of 3*d* electrons.[36]

Note that the UPS of TiFe is a single band with a maximum at about 1 eV. In the other cases UPS has a two band shape. The band that is located close to the Fermi level practically does not change its energy position by variation of the *M* type and the other one moves to the bottom of the valence band as the *M* atomic number increases. As the conditions of excitation of both partners are the same in titanium based compounds with late 3*d* metals, one may believe the UPS reflects the total density of states. Then the band which changes its energy position as the *M* atomic number increases primarily reflects the *M d* band. The low energy peak near E_F should correspond to the Ti *d* band which we failed to observe in XPS.

We could think that the surface contribution can affect the UPS shape because of the less electron escape depth in comparison with XPS (~5.4 and 18 A, respectively). The surface specific nature of the surface emission is indicated by its extreme sensitivity to gas contaminations relative to other spectral features which are known to be a bulk origin. Contamination as it follows from all known

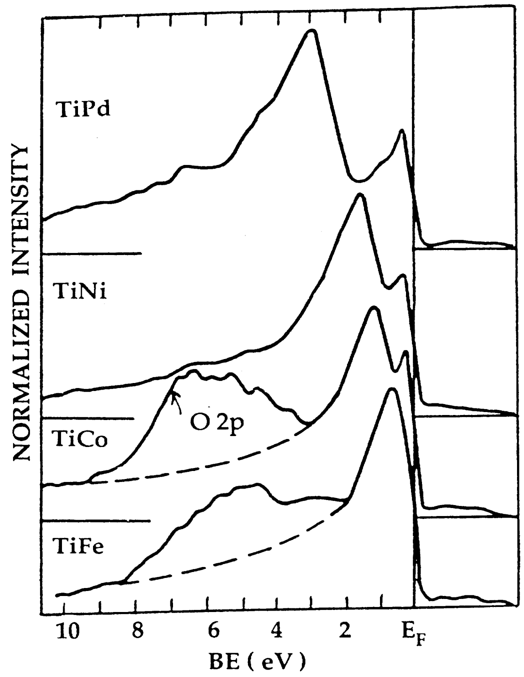

FIG. 10. UPS from TiFe, TiCo, TiNi, and TiPd. 2*p* band of oxygen is pronounced in spectra when sample surfaces were subjected only to ionic etching without a preliminary chemical one.

investigations, smoothes or even destroy the surface DOS picture of metals because of saturating the "dangling bonds." Analyzing Fig. 10 we can see that samples of TiPd and TiNi having clean surfaces have the same spectrum structure as TiCo with contaminated surface, except for O 2*p* band. This means that the observed UPS structure reflects only the bulk DOS which is not affected by contamination.

It is necessary to note that the energy shift (ΔE_d) of the *M* *d* band, passing from an elemental state to the compound, practically coincides with the energy difference in the location of the *M* and Ti *d* subbands in Ti*M* compounds.

Let us compare the UPS and XPS with DOS curves[37] for quasibinary Ti(Ni,*M*) compounds (Fig. 11). At the right side of the Fig. 11 the density of states are presented. At the left the same curves broadened by a 0.85-eV Gaussian spectrometer function together with experimental spectra are shown. It can be seen that at binding energies less than 3 eV the $N(E)$ shape is better reproduced by UPS. In contrast, at $E_B > 3$ eV we see better agreement between XPS and the DOS curve. We know that the difference between UPS and XPS shape is caused first of all by the difference of *d* photoelectron cross section of the two partners. But what is the reason of the difference in shape of the Pd *d* band in UPS and XPS? The unpronounced low-energy part of the Pd *d* band ($4d_{3/2}$ states) becomes an independent peak at 4 eV in XPS. As follows from Ref. 38 the increase of excitation energy from 21.2 eV (He I) to 40.8 eV (He II) leads to significant intensity increase in the low-energy part of the Pd ultraviolet spectrum because of enhancement of the $4d_{3/2}$ photoelectron cross section. Thus, the difference in the Pd *d*-band shape in UPS and XPS is also the result of difference in cross section, in this case, between the Pd 4*d* spin-doublet components.

The method used by the authors in Ref. 37 does not provide the opportunity to calculate the local density of states in quasibinary compounds. However, based on the analysis of the phase shifts, one can conclude that the

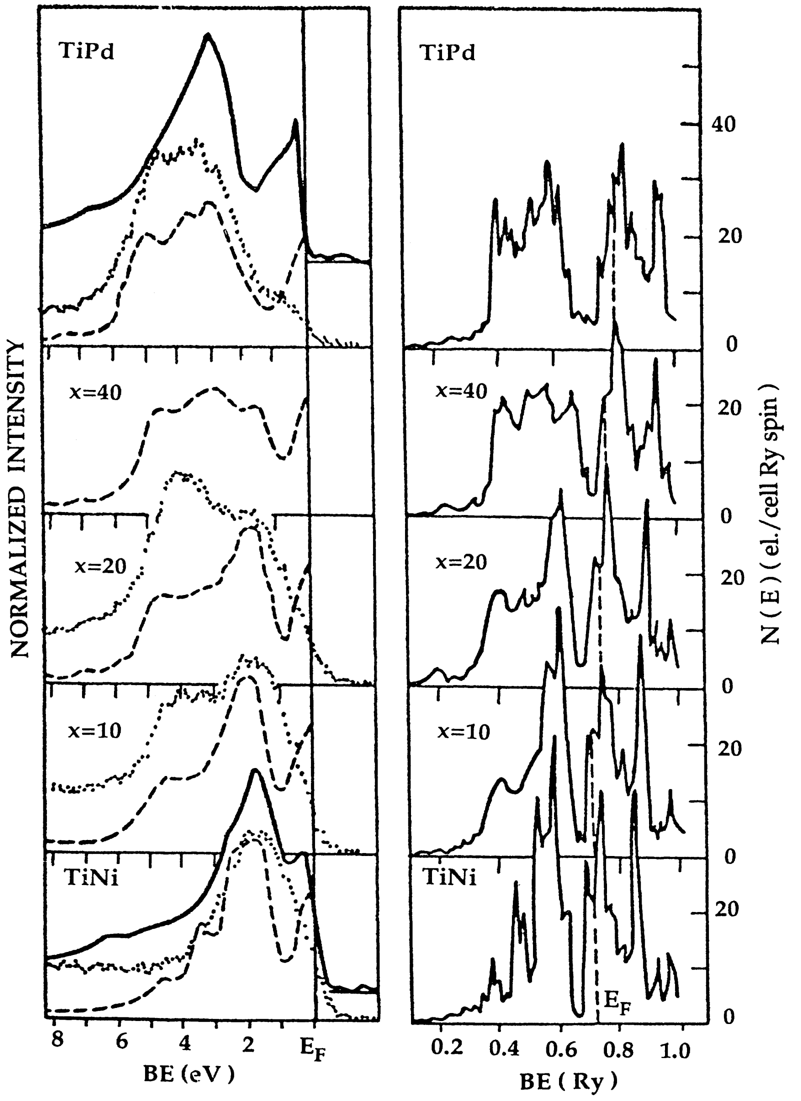

FIG. 11. Left panel: comparison of XPS (dotted line) and UPS (solid line) VB spectra from $Ti_{50}(Ni_{50-x}Pd_x)$ compounds with the total DOS (Ref. 37) broadened by 0.85-eV Gaussian function. Right panel: DOS calculated in Ref. 37.

high-energy band of $N(E)$ in the occupied part in the vicinity of E_F is caused by Ti d states, which is in agreement with experimental data and the recent theoretical calculations of electronic structure.[39] The analysis of the theoretically calculated band structure shows that the energy gap between Ti and M d bands increases passing from TiNi to TiPd. This may be considered as a result of enhancement of the ionic contribution to the interatomic bond.

It follows from the results presented here, that in Ti-based compounds with late transition metals, the band caused primarily by the Ti d states is located in the vicinity of the Fermi level. What about the actual density of states of this subband? Because of the similarity in the d photoelectron cross section of the two partners in TiNi, UPS correctly reproduces the $N(E)$ shape. Taking into account that the Pd d-electron cross section is several times larger than that of Ti we can suppose that $N(E)$ value in the E_F vicinity in TiPd is comparable to the DOS of the Pd d subband located deep in the valence band. This result is in agreement with some theoretical calculations,[37] but in contradiction to others.[40]

There exists a rather uncommon method for the qualitative estimation of Ti d-state contribution to $N(E_F)$ using the $K\alpha_1(2p\text{-}1s)$ emission line.[41] The width of the line depends on variations of the $2p_{3/2}$ level multiplet structure. This multiplet structure appears in the final state as a result of $2p$ electron interaction with uncoupled $3d$ electrons which have fallen from the conduction band and are responsible for the $2p$ hole screening. The localized $3d$ spin density (the Friedel level), caused only by the $2p$ hole potential, polarizes, in turn, the conduction electrons like a magnetic field and influences the $K\alpha_1$ width. As a consequence the temperature dependence of the Ti $K\alpha_1$) linewidth is similar to that of paramagnetic susceptibility in martensitic-transformation region in TiNi.[32,33]

The investigation of TiM compounds[32] has shown that the Ti $K\alpha_1$ linewidth gradually increases with the M atomic number (Fig. 12). By complete substitution of Pd for Ni the latter value reaches 1.73 eV. As the $K\alpha_1$ width is a measure of uncoupled spin density in the conduction band, its variation is a measure of the Ti d states at the Fermi level. In other words, we actually observe an increase of Ti contribution to the DOS at E_F as the M atomic number increases.

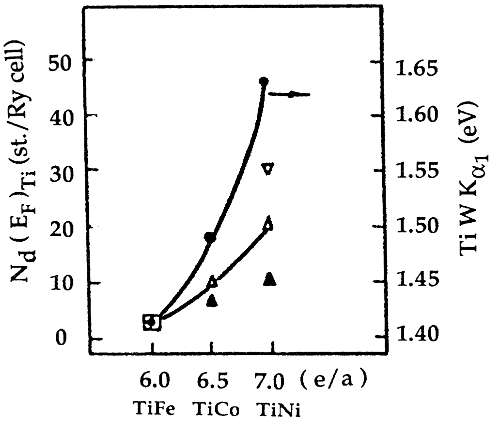

FIG. 12. Comparison of dependencies of Ti $K\alpha_1$ width (W) with the local Ti d contribution to $N(E_F)$ vs average electron number per atom (e/a). Results of theoretical calculations have been taken from Refs. 14, 42, and 43 (□) for TiFe; from Refs. 18, 42 (△), and 44 (▲) for TiCo; from Refs. 15 (▽), 20 (▲), and 23 (△) for TiNi.

Figure 12 also shows the results of theoretical calculations for the Ti d density of states at the Fermi level, $N_d(E_F)_{Ti}$. As for TiFe, all know theoretical calculations coincide with each other,[14,42,43] therefore we can tie the width of the $K\alpha_1$ line and the $N_d(E)_{Ti}$ curve at the electronic concentration of TiFe. Any deviation of the theoretical $N_d(E_F)_{Ti}$ calculations from the Ti $K\alpha_1$ width indicates the inadequacy of the former. Evidently, the greatest scattering of theoretical data is observed in the case of TiNi. The calculations by Papaconstantopoulos,[15] predicting the dominant of the Ti d contribution to the $N(E_F)$ is the closest to the experimental data in contrast to that of Bolezkaya.[23]

F. Electronic structure and martensitic transformation

The preceding sections were devoted to the study of the valence-band structure in equiatomic Ti compounds. It was established that in the sequence of isomorphic compounds the structure of the valence-band changes regularly with atomic number. In the next section it will be shown that this determines the interatomic bond and stability. If the valence-band structure is so important for phase stability, we may suppose it will change significantly at phase transformations. Having at our disposal methods which allow us to perform temperature investigations, we have studied the electronic structure in different phase states.

A previous investigation of TiNi[12,13] showed that martensitic transformation is accompanied by a small intensity redistribution and shift of subbands with respect to E_F by ~0.2 eV. Since ionic etching was used in our earlier work to clean samples, we repeated this experiment again, using mechanical cleaning, a more foolproof method. It turned out that the results for TiNi agree with each other very closely. We also performed research with different binary and ternary Ti compounds. Because high-temperature research requires specific precautions, most experiments have been conducted using alloys with martensitic-transformation temperatures close to room temperature.

Now we present some of these results. Figure 13 shows the XPS of the ternary Ti(Ni,Au) alloy in the $B2$ and $B19$ structures. As can be seen, the main features of the valence band remain unchanged upon martensitic transformation. However, there occurs a redistribution of intensity between Au spin-doublet components simultaneously with increase of the Ni band with respect to that of Au. The difference curve shows the greatest differences are observed in the middle of the main subbands.

Evidently, new energy gaps appear in the low symmetric orthorhombic $B19'$ phase. These gaps weaken the

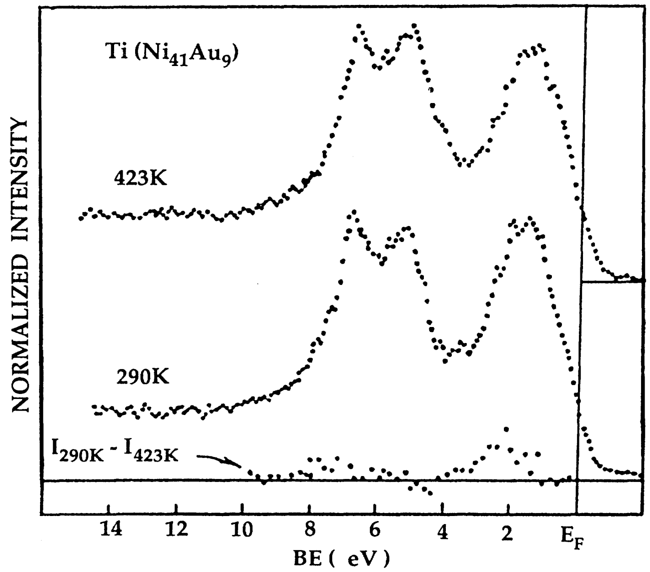

FIG. 13. XPS VB from Ti$_{50}$(Ni$_{41}$Au$_9$) in $B2$ (423 K) and $B19$ structure (290 K).

s-d hybridization and thereby cause strengthening of the d character and increase of XPS intensity at corresponding energy. In this case, as in all others, the 0.2 eV narrowing of the XPS at the half maximum intensity, as well as the shift of both main subbands from the Fermi level are observed in the low-temperature phase. The observed d-band narrowing is in agreement with the volume increase in the $B19$ martensite structure.

The energy of Ti and Ni $2p$ levels within the limits of experimental accuracy (± 0.1), does not change at martensitic transformation of TiNi. However, in ternary alloys another core-level behavior was discovered: The Ti and Ni $2p_{3/2}$ level energy decreases by 0.1–0.2 eV and that of Pd $3d_{5/2}$ and Au $4f_{7/2}$ increase by the same value in the low-temperature phase.

In distinction from other alloys we have studied in which a small decrease of XPS ($\sim 10\%$) at the Fermi level was detected, in the example presented here, the E_F situation is practically unchanged upon the martensitic transformation.

The considered results give us information about the second and third components. UPS are of particular interest for the study of the Ti electron-density distribution. Figure 14 presents the UPS normalized to the intensity of the main maximum. The result of the phase transformation is a distinct enhancement of the Ti subband in the E_F neighborhood. The latter effect, more or less pronounced, is reproducible in all experiments. The Pd maximum shifts toward the E_F by 0.2 eV in the $B19$ structure. These data indicate the Ti d states experience the largest change at the martensitic transformation. Based on this we have studied the Ti $CC'V$ Auger spectrum in both phases. Auger spectra will be considered in detail in another paper.[16] Here we are only concerned with the phase-transformation effect. As the $CC'V$ transition involves only one electron from the valence band (Auger electron), its shape must reflect the structure of the local d density of states at the Ti sites.

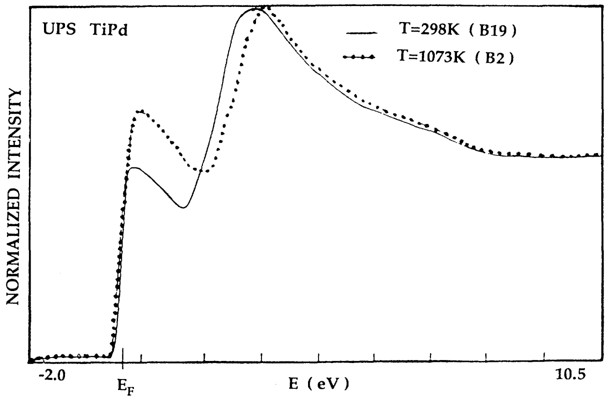

FIG. 14. UPS VB from TiPd in $B2$ (1073 K) and $B19$ (298 K) structure.

It can be seen that the Ti $L_3M_{2.3}M_{4.5}$ spectrum has the structure of two bands separated by ~ 3 eV (Fig. 15), which is close to the energy difference between the two bands in UPS. The larger intensity of the high-energy maximum which is closer to E_F means that the intensity of $N(E)$ at E_F strongly exceeds that of the middle of the valence band. In order to make a comparison, both spectra should be normalized to the intensity of the main maximum. However, it is obvious that as a result of the phase transformation, the intensity of the main maxima increases with respect to the low energetic maximum, which is in agreement with the UPS data.

It is necessary to note that the electronic spectra do not resolve the change of situation at the Fermi level at the martensitic transformation yet. However, according to optical[45] and magnetic susceptibility data[2,46] the martensitic transformation $B2$-$B19'$ in TiNi is accompanied by significant decrease of d density of states at E_F and as a result a new pseudogap develops around Fermi level.

Let us now try to estimate the possibility of d-s transfer at martensitic transformation. The negative sign of volume change in the high-temperature $B2$ phase in TiNi can be considered in terms of high pressure. In this case the 0.6% decrease in the volume of the high-temperature

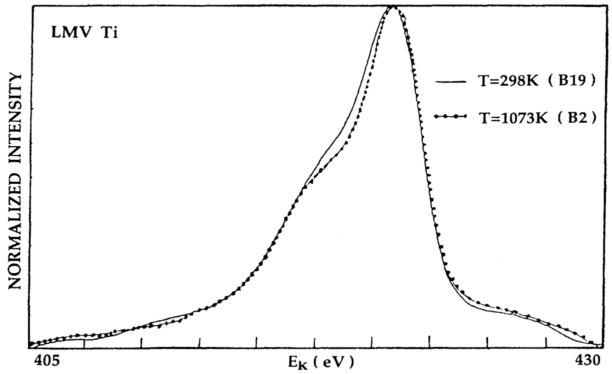

FIG. 15. $L_3M_{2.3}M_{4.5}$ Auger spectrum from Ti in TiPd in different structural states.

$B2$ structure in comparison with $B19'$ in TiNi may indicate increase of the *d* electron number due to *s*-*d* transition. This transition arises from the fact that the spatially extended *s* and *p* states feel the effect of high-pressure more strongly than do the localized *d* states. Thus, the corresponding *s* and *p* energy bands, rise in energy faster than do the *d* bands, transferring electrons from *s* and *p* states to *d*-like states in the process. As the early transition metals are very sensitive to high pressure in contrast to the late ones[47] electron reconstruction will mainly affect the Ti *d* electrons in TiNi. Since the martensitic transformation $B2$-$B19'$ in TiNi is accompanied by ~ 0.2-eV shifts of core levels of components we may assume the *s*-*d* charge transfer of only a few hundred electrons per atom. Actually it can be the consequence of the change of the character of *sd* hybridization.

IV. INTERATOMIC BOND AND STABILITY OF $B2$ STRUCTURE IN TI-BASED COMPOUNDS

Based on the results of the presented research, we now try to draw a general picture of the electronic structure and the interatomic bond evolution in Ti*M* compounds and link them with the $B2$ phase stability. We will start from TiFe, which is stable in CsCl structure until 0 K. The Ti *d* band does not display itself separately from the *M d* band in UPS in this case. This means that in TiFe where the *d* orbitals of both components are partially occupied, the hybrid *d*-*d* bond is formed. As the *d* band occupancy in pure Ti and Fe is such that practically only the bonding portion of the valence band is occupied, the cohesive force is strongest in TiFe among the compounds investigated, and the $B2$ structure is preserved down to helium temperatures. In this case the negative sign of $K\alpha_1$ shifts for both partners indicates extraction of the charge into the interstitial sites.

Experimental data show that increase of the *M* atomic number along a period and through a column leads to separation of the maxima, as well as of the centroids, of partner *d* bands in the filled part of the valence band. Obviously, this causes the decrease of the *d*-*d* overlap and accordingly the covalent bond weakening. This process is accompanied by strengthening of the ionic contribution. As the direction of the charge transfer is concerned, it is not possible to get such information from the core-level shifts because the final value of core-level shift is caused by the charge which is drawn off from the atom sites into the interstitial ones and by the charge, which really transfers from one component to another.

Based on the concept of *d*-*d* hybridization, the 40–60 % $L\alpha_{1,2}$ (transition $3d$-$2p$) integrated intensity enhancement of both components by alloying,[9] which cannot be connected with the corresponding occupancy increase of the local *d* bands, ought to be considered as a result of "effective" *d* occupancy increase caused by the energy overlap of partner *d* bands. In other words it is due to covalency. The larger $L\alpha_{1,2}$ intensity increase observed in TiFe compared to TiCo and TiNi indicates larger *d*-*d* overlap.

To finish the discussion of the interatomic bond in this section let us turn to Fig. 16, which can help us understand another contribution to the covalent bond in Ti*M*. This figure presents the change of integrated intensity of $L\alpha_{1,2}$ and $K\beta_{2,5}$ emission bands upon passing from an elemental state to a compound.[9] The $L\alpha_{1,2}$ spectrum only reflects the $3d$ density. The $K\beta_{2,5}$ spectrum, however, includes both the dipole transition $3d$-$1s$ and the quadruple $4p$-$1s$. Note the correlation in behavior of the first and third and the second and fourth curves, respectively, shown in Fig. 16. One can surmise the observed correlation indicates a change in the interaction of $3d4p$ Ti electronic states with $3d$ *M* (first and third curves) and $3d4p$ *M* states with $3d$ Ti (second and fourth curves). Then the reduction of the integrated intensity of the Ti $K\beta_{2,5}$ and *M* $L\alpha_{1,2}$ spectra in the presented compounds reflects a weakening of $4p3d$ Ti-$3d$ *M* covalent bond which is accompanied by the destabilization of $B2$ structure.

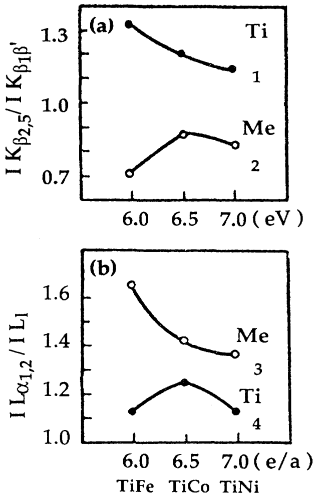

FIG. 16. Change of integrated intensities of $L\alpha_{1,2}$ and $K\beta_{2,5}$ emission bands passing from an elemental state to Ti*M* compounds for Ti and *M*.

Thus, we have followed the evolution of the valence-band structure in Ti*M* compounds. We came to the conclusion that as the atomic number of *M* increases (both within the same period and along the same column), its *d* states become more localized, the maximum and the center of gravity of the *d* bands shift towards the bottom of the valence band and the *M* contribution to the density of states at the Fermi level degrades. The larger the *M d* subband shift towards the bottom of the valence band (ΔE_d) is, the more the *d* resonances of the two partners are energetically separated. The partner *d* resonance separation practically coincides with ΔE_d because the main maximum of the Ti *d* band remains in the E_F vicinity (where the *d*-band maximum of *M* in the elemental state was located) upon passing from the elemental state to the compound in contrast to the main maximum of the *M d* band. The decrease in overlap of the partner subbands results in weakening of the covalent bond between the components of the alloy and, thus, destabilization of the $B2$ phase.

While the contribution of *M d* electrons to the DOS at E_F decreases, the Ti *d* portion increases to such an extent that in TiPd and TiAu the *M* contribution to $N(E_F)$ is almost negligible.

The strong energy localization of the *M d* band, which according to positron annihilation data is accompanied by spatial localization,[17] indicates a tendency of the *d* bands, at least among the last transition metals, towards atomization. This effect is pronounced in Auger spectra of Ni and Pd.[16] Thus, due to the localization of the Ni *d* band, the directed *d* bond is formed only by the Ti *d* electrons. Based on the present analysis we suggest that the nearest neighbors along the [111] chains are bound by *d* Ti-*p* Ni hybridization, while the bonding of second and third neighbors is due to the *d* Ti-*d* Ti hybridization, similar to that in βTi. The *d-d* bond between Ni atoms should be extremely weak. This actually means that the Ti-Ti and Ti-Ni interaction dominates the interatomic bonding in TiNi. This point of view is in agreement with calculations of force constants in TiNi.[21]

The established regularities in the interatomic bond are strongly supported by Fig. 17, in which the $B2$-$B19(B19')$ martensitic-transition temperature M_s for binary Ti*M* and quasibinary Ti(Ni,*M*) compounds versus the cubic lattice parameter is presented. The M_s's of all the $B2$ compounds can be fitted by a single parabolic curve. TiFe, the compound with the most pronounced covalency, has the smallest lattice parameter. M_s increases from 0 K to the temperature of the allotropic β-α transition in Ti. This reflects the fact that the cubic phase stability in pure Ti and Ti-based $B2$ compounds may have the common nature. Upon varying the lattice parameter, we can identify distinct areas where different sets of martensitic transition take place. So for $a > 3.05$ Å we observe the simple $B2$-$B19$ transition and for $a < 3.05$ A we observe the sequence of transformations $B2$-R-$B19'$.

It is characteristic that the rhombohedral R phase (T_R temperature) occurs in the ternary TiNi-based alloys only upon lattice compression with respect to cubic TiNi phase. In fact, this is the same situation as with the ω phase in Ti-based bcc alloys when the ω phase is initiated either by hydrostatic pressure applied to pure Ti or by lattice parameter decrease due to alloying with V, Cr, Mn, or Fe. This means that the effect of impurities on lattice parameter and phase stability is similar to the effect of pressure in these cases.

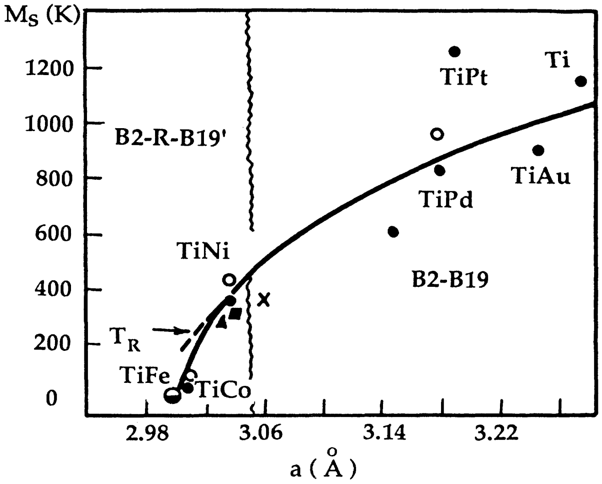

FIG. 17. The start temperature of $B2$-$B19(B19')$ martensitic transformation vs lattice parameter in $B2$ structure. All lattice parameters have been extrapolated to the same temperature (1100 K). △—1 at. % Fe, ■—8 at. % Pd, *x*—15 at. % Cu, and ▼—25 at. % Pt substituting Ni in $\mathrm{Ti}_{50}(\mathrm{Ni}M)_{50}$ compounds. ○—calculated using empirical formula for M_s.

To finish this discussion we will return to the compounds with noble metals. As can be seen in Fig. 17, the M_s temperature for TiAu falls on the same line which is characteristic for transition-metal compounds. This supports our consideration of Au as a metal with partially unfilled *d* band. In contrast to TiAu, the compounds TiCu and TiAg do not exist in the CsCl structure. The differences among noble metals causing this situation can be understood as a result of different number of delocalized *d* electrons which are responsible for the directed covalent bond. Increase of this number passing from Ag to Cu and Au (Ref. 48) creates more favorable conditions for the *dd* covalent bond formation and for the $B2$ phase stability.

Thus, we have shown that the main factor affecting the stability of both TiNi and other $B2$ Ti-based compounds is the occupancy of the *d* bands and the resulting *d-d* hybridization which governs the interatomic interaction. Analysis of the evolution of *d* bands of the components upon alloying enables one to form a sequence of compounds:

TiFe-TiCo-TiNi-TiPd-TiPt-TiAu-TiCu-TiAg ,

along which the stability of the $B2$ phase decreases, correlated with the localization of the *M d* band and with the weakening of the *d-d* and *d-p* directed bonds between different kinds of atoms.

Based on these empirical correlations, discussed in this paper we suggest the following phenomenological formula for the temperature of the martensitic transformation in Ti*M* compounds:

$$M_s = M_s(\mathrm{Ti})(a_{\mathrm{Ti}M}/a_{\mathrm{Ti}})^{1/2}(\Delta E_d/W_M) \times [N_d(E_F)_{\mathrm{Ti,B2}}/N_d(E_F)_{\mathrm{Ti,bcc}}] ,$$

where $M_s(\mathrm{Ti})$ is the temperature of the allotropic β-α transformation in Ti, **a** is the lattice parameter in the cubic structure (either $B2$ or bcc), ΔE_d is the shift of the maximum of the *M d* band in the compound with respect to that in the elemental state, W_M is the *M d* band width in the Ti*M* compound, and $N_d(E_F)$ is the Ti *d* DOS at E_F in the $B2$ and bcc structure.[49] The M_s temperatures calculated using this formula (the open circles) agree well with the experimental data. The parameters in the formula are the fundamental parameters of the alloy theories and control interatomic bonding. To be more correct, we should write the above formula for the temperature of equilibrium of two phases $T_0 = (A_s + M_s)/2$ instead of M_s. However, because the temperature hysteresis in equiatomic Ti*M* compounds is small, not exceeding 40°, one can use M_s.

The above equation enables one to perform a "smart" analysis of the effect of alloying on M_s. The main parameter that affects M_s in equiatomic Ti*M* compounds is the factor $\Delta E_d/W_M$, which controls the *d*-*d* hybridization. Upon dilute alloying in Ti(Ni,*M*) alloys, when an impurity forms local resonance, the *d* DOS widens due to alloying disorder and M_s is controlled mainly by the lattice parameter and $N_d\ (E_F)_{\mathrm{Ti}}$.

In quasibinary compounds, the bonding is stronger due to enhancement of hybridization, either *d*-*d* (if the alloying metal's atomic number is less than that of Ni) or *sp*-*d* (upon substitution of *sp* or noble metals for Ni). In both cases the quantum mixing of the orbitals leads to suppression of the tendency towards shear transformations. The faster decrease of the M_s temperature which is observed by substituting Cr for Ti (Ref. 46) is understandable, now, as a reaction to the larger increase in *d*-*d* covalency, since Cr has the greatest possible number of delocalized *d* orbitals suited for this bond.

The effect of interstitial impurities on M_s may also be explained by the above consideration making use of quantum-chemical calculations of electronic structure of interstitial impurities in transition metals.[50] The *p* elements (C,O), as substitutional impurities, have to stabilize the *B*2 phase by forming *p*-*d* bonds. Hydrogen, an *s* element, forms mostly *s*-*p* hybrids and, thus, its electron does not mix with *d* orbitals. A strong *d* resonance at E_F in titanium hydrides may also be expected in TiNi-based hydrides, since the Fermi level of the latter is dominated by the Ti *d* states. As a result, the rise of M_s and destabilization of the *B*2 structure will be observed.

V. CONCLUSION

The main data concerning valence-band evolution in Ti*M* compounds are presented in this paper. Auger spectroscopy[16]and positron annihilation data[17] provide further information about specific details in electronic structure. However, global regularities are already clear. Such a detailed consideration of original materials is presented in our hope that they may be of particular interest themselves and can be used not only as criteria for the validity of theoretical calculations but also as a basis for the development of an exact theory of phase stability in transition-metal compounds.

Based on the picture of the valence-band evolution, a model of interatomic bond and a phenomenological description of *B*2 phase stability of Ti-based compounds have been presented. This model does not pretend to be perfect. It is only an attempt to explain the *B*2 phase stability in shape memory alloys in the absence of developed theoretical approaches. It is remarkable that it works and clarifies many things which earlier were not understandable. For example, the reasons for *B*2 phase stability variation with *M* atomic number, the distinction between noble and transition metals that determine the homogeneity region of *B*2 compounds, and the most importantly, the influence of alloying on the temperature of the martensitic transformation.

Due to localization of the Ni *d* band, the Ti *d* electrons give decisive contribution to the interatomic bond and the domination of these electrons at the Fermi level results in additional renormalization of the elastic moduli, the phonon frequencies, and the electron-phonon interaction. This explains why the stability of the *B*2 titanium-based compounds, controlled by the C' modulus and the transverse-acoustic (110) Brillouin-zone boundary phonons, is governed mostly by the Ti *d* states.[51]

As expected, the same fundamental parameters control the phase stability in both pure transition metals[52,53] and in their compounds. They are the *d*-band occupancy of the two components which determines the energy resonance differences and the *d*-band width, thereby the bond character and the Fermi level density of states. The role of the Ti *d* peak in the Fermi-level vicinity is dual. On one hand, it provides the tendency toward displacive transformations, and on the other, it stabilizes the *B*2 structure due to the electron entropy contribution to the total energy with temperature increase.

The reconstruction of the DOS curve and decrease of $N(E_F)$ in the low-temperature phase in all cases investigated indicates that the guiding force of martensitic transformation may be the gain in one-electron energy.

ACKNOWLEDGMENTS

We thank A. Lotkov, A. Zakharov, and V. Kachin for their help in experiment arrangement; A. Korotaev, B. Harmon, K. M. Ho, G. Krasko, and A. Petridis for their support and encouragement. It is also a pleasure to acknowledge discussions with A. A. Baturin, R. L. Barinski, and Dr. I. Kulikova. This work was supported and financed by the Russia Budget Program of Fundamental Research, in Siberian Physical Technical Institute in Tomsk, U.S. Department of Energy under Exchange Visitor Program No. P-1-732, and partially supported by the Director for Energy Research, Office of Basic Energy by Iowa State University under Contract No. W-7405-Eng-82.

---

[1] S. A. Shabaloskaya, A. I. Lotkov, and A. A. Baturin, Phys. Met. Metallogr. **56**, 67 (1983).

[2] C. M. Hwang, M. Meichle, M. B. Salamon, and C. M. Wayman, Philos. Mag. **47**, 9 (1983).

[3] M. Keil, M. Müllner, and W. Weber (unpublished).

[4] G. L. Zhao, T. C. Leung, and B. N. Harmon, Phys. Rev. B **40**, 7999 (1989).

[5] J. R. Cuthill, M. I. McAlister, and W. L. Williams, J. Appl. Phys. **39**, 2240 (1968).

[6] A. S. Shulakov, T. M. Zimkina, V. A. Demichev, and V. A. Nagorni, Sov. Solid State Phys. **15**, 3598 (1973); these results have been reproduced using other structural attestated samples by A. S. Shulakov and S. A. Shabalovskaya (unpublished).

[7] V. P. Mamko, Ph.D. thesis, Institute of Metal Physics, Kiev, Ukranian, 1976.

[8] J. F. Holiday, *Soft X-ray Band Structure of Metals and Materials* (Academic, New York, 1980).

[9]V. V. Nemoshkalenko, *X-ray Emission Spectroscopy of Metals and Alloys* (Naukova Dumka, Kiev, Ukranian, 1972).

[10]H. Föll, Z. Phys. B **26**, 329 (1977).

[11]E. Källne, J. Phys. F Metal Phys. **4**, 167 (1974).

[12]S. A. Shabalovskaya, A. I. Lotkov, and I. I. Sasovskaya, Solid State Commun. **32**, 735 (1979).

[13]S. A. Shabalovskaya, A. G. Narmonev, A. I. Lotkov, and A. I. Zakharov, Physics of Metals and Metallography **51**, 33 (1981).

[14]D. A. Papaconstantopoulos, Phys. Rev. B **11**, 4801 (1975).

[15]J. D. Shore and D. A. Papaconstantopoulos, J. Phys. Chem. Solids **45**, 439 (1984).

[16]S. A. Shabalovskaya, O. P. Ivanova, and A. P. Dementjev, Surf. Sci. **251/252**, 377 (1991).

[17]S. A. Shabalovskaya and A. A. Baturin, Solid State Commun. (to be published).

[18]I. Kübler, J. Magn. Magn. Mater. **15**, 859 (1980).

[19]J. D. Scofield, J. Electron Spectrosc. Relat. Phenom. **8**, 129 (1976).

[20]I. I. Naumov, A. G. Sheihulov, and O. I. Velikhohatni, Zh. Eksp. Teor. Fiz. (Sov. Phys. JETP) (to be published).

[21]M. Keil, Diplomenarbeit, Institut fur Kernphysik, Johann-Wolfgang Goethe Universität, Frankfurt, 1989.

[22]G. L. Zhao and B. N. Harmon, Phys. Rev. B **48**, 2031 (1993).

[23]T. K. Boletskaya, Ph.D. thesis, Tomsk State University, Tomsk, 1984.

[24]F. Steiner, M. Schmidt, and S. Huffner, Solid State Commun. **49**, 1081 (1984).

[25]L. F. Mattheis and R. E. Dietz, Phys. Rev. B **22**, 1663 (1980).

[26]P. Steiner, M. Schmidt, and S. Huffner, Solid State Commun. **35**, 493 (1980).

[27]W. Lambrecht, Phys. Rev. B **34**, 7421 (1986).

[28]F. U. Hillerbrecht *et al.*, Phys. Rev. B **27**, 2179 (1983).

[29]T. K. Hatwar and D. Chorpe, Surf. Interface Anal. **7**, 93 (1985).

[30]V. L. Moruzzi and P. Oelhafen, Phys. Rev. B **27**, 2049 (1983).

[31]H. B. Michaelson, IBM J. Res. Dev. **22**, 72 (1978).

[32]R. L. Barinsky, O. P. Kosheleva, S. A. Shabalovskaya, and I. M. Kulikova, Sov. J. Inorg. Chem. **35**, 107 (1990).

[33]R. L. Barinsky, I. V. Kosheleva, and I. M. Kulikova, Phys. Met. Metallogr. **67**, 491 (1989).

[34]B. M. Mogutnov and L. A. Schwarzman, Sov. J. Phys. Chem. **1**, 568 (1980).

[35]J. Tersoff, L. M. Falikov, and D. R. Penn, Solid State Commun. **32**, 1045 (1979).

[36]J. J. Yeh and I. Lindau, At. Data Nucl. Data Tables **32**, 1 (1985).

[37]V. P. Lapin, V. E. Egorushkin, S. A. Shabalovskaya, and O. P. Ivanova, Solid State Commun. **73**, 471 (1990).

[38]P. Oelhafen, M. Liard, and H. Guntherodt, Solid State Commun. **30**, 641 (1979).

[39]Y. G. Ding, C. T. Chan, and K. M. Ho, Bull. Am. Phys. Soc. **38** (1) 307 (1993).

[40]M. L. Miller and V. N. Antonov, Dokl. Akad. Nauk SSSR **292**, 82 (1987) [Sov. Phys. Dokl. **32**, 43 (1987)].

[41]R. L. Barinsky, I. M. Kulikova, and E. P. Shevchenko, Izv. Akad. Nauk SSSR, Ser. Fiz. **46**, 724 (1982).

[42]G. Shadler and F. Weinberger, J. Phys. F **16**, 27 (1986).

[43]E. Z. Da Silva *et al.*, Phys. Rev. B **36**, 3015 (1987).

[44]V. V. Kalchikhin, S. E. Kulikova, and O. N. Murishnikova, Sov. Phys. J. Izvestija vuz. Fizika, Archival No. 244-890 (Jan. 15, 1990).

[45]I. I. Sasovskaya, S. A. Shabalovskaya, and A. I. Lotkov, Zh. Eksp. Teor. Fiz. **77**, 2341 (1979) [Sov. Physics JETP **50**, 1128 (1979)].

[46]S. A. Shabalovskaya, Phys. Status Solidi B **132**, 327 (1985).

[47]J. A. Moriarty, Phys. Rev. B **45**, 2004 (1992).

[48]D. O. Welch and N. G. Lynn, Phys. Status Solidi B **77**, 277 (1976).

[49]G. L. Krasko (private communication).

[50]A. L. Ivanovsky, D. L. Novikov, V. I. Anisimov, and V. A. Gubanov, Zh. Strukt. Khim. **30**, 381 (1989).

[51]S. A. Shabalovskaya, in *Shape Memory Materials and Phenomena*, Fundamental Aspects and Application, edited by S. T. Liu, H. Kunsman, K. Otsuka, and M. Wuttig, MRS Symposia Proceedings No. 246 (Materials Research Society, Pittsburgh, 1992), p. 247; (unpublished).

[52]D. B. Pettifor, J. Phys. C **3**, 367 (1970).

[53]M. Sigalas, D. A. Papaconstantopoulos, and N. C. Bacalis, Phys. Rev. B **45**, 5777 (1992).